Meas. Sci. Technol. **10** (1999) 845–852. Printed in the UK PII: S0957-0233(99)01978-5

Diode laser measurements of concentration and temperature in microgravity combustion

Joel A Silver and Daniel J Kane

Southwest Sciences Inc., Suite E-11, 1570 Pacheco Street, Santa Fe, NM 87505, USA

E-mail: jsilver@swsciences.com

Received 19 February 1999, in final form and accepted for publication 7 April 1999

Abstract. Diode laser absorption spectroscopy provides a direct method of determinating species concentration and local gas temperature in combustion flames. Under microgravity conditions, diode lasers are particularly suitable, given their compact size, low mass and low power requirements. The development of diode laser-based sensors for gas detection in microgravity is presented, detailing measurements of molecular oxygen. Current progress of this work and future application possibilities for these methods on the International Space Station are discussed.

Keywords: gas concentration, temperature, diode lasers, microgravity combustion

1. Introduction

Understanding the physical phenomena controlling the ignition and spread of flames in microgravity has importance for space safety as well as for characterizing dynamical and chemical combustion processes which are normally masked by buoyancy and other gravity-related effects. In the absence of buoyancy, low gravity flames can be examined closely to study the effects controlling ignition, quenching and blowoff, flame spread, size and temperature, soot formation and other phenomena.

Unfortunately, combustion is highly complicated by fluid mechanical and chemical kinetic processes. This complexity requires the use of numerical modelling to make comparisons with carefully designed experiments. Given the development of these detailed theoretical models, more sophisticated diagnostic methods are needed to provide the kind of *quantitative* data necessary to characterize the properties of microgravity combustion as well as to provide accurate feedback to improve the predictive capabilities of the models.

Quantifying local gas temperatures and multiple species concentrations on a rapid time scale is desirable, yet for many years microgravity research has been limited to capturing flame emissions on photographic or video media, laser Schlieren imaging, or intrusive thermocouple measurements for these critical data. Few 'robust' methods are available due to the severe limitations on instrument size, weight, safety, power and cooling requirements suitable for use in drop towers, sounding rockets, airplanes and space flight.

Research to develop diode laser-based absorption methods to overcome these limitations is reported in this paper. The detection of molecular oxygen in both thin solid sheet flames and candles is demonstrated. The drawbacks of the current systems and subsequent improvements needed are detailed. Our progress in developing robust gas sensors suitable for use in drop towers, and ultimately for the International Space Station, is presented.

2. Background

The development of non-intrusive diagnostics for microgravity combustion research is relatively new. The need for accurate quantitative measurements of species concentration and temperature, resolved in both time and space, is obvious. Yet unlike in conventional combustion diagnostics, the tools suitable for low-g measurements were not available. Solid state diode lasers that operate in the visible or near-infrared spectral regime are capable of meeting the many restrictions imposed upon experimental systems used in microgravity research. With the increasing availability of these lasers at wavelengths corresponding to absorption lines of major combustion species, we can finally begin to perform quantitative measurements important to unravel the complexities of combustion in the absence of gravity.

Microgravity research depends on experiments performed in drop towers, low-g parabolic airborne flights, and in a few selected cases, sounding rockets or Space Shuttle flights [1]. Instrument size, reliability, weight, power and ruggedness are critical issues that limit the usefulness of most laser-based diagnostic methods. Most microgravity platforms are powered by modest sized batteries. Other important factors include fire and eye safety. The development of laser sources has focused primarily on drop tower

0957-0233/99/100845+08$30.00

measurements, as these are the most pervasive platform for microgravity studies.

Diode lasers are a natural choice for use under the severe conditions of low gravity. Reliable, simple solid state operation at low power satisfies many of these restrictions. In addition, these lasers can be fabricated to detect most major and minor combustion species, with the goal of simple interchangeable units being quite realistic. The use of lasers for absorption measurements allows very sensitive detection with extremely rapid response times in an inexpensive package.

The first diode lasers which reliably exhibited single-mode (wavelength) operation were mid-infrared lead-salt lasers that required cryogenic cooling [2, 3]. While direct absorption in the mid-infrared may exhibit sufficient sensitivity for detecting many species, these systems are not suitable for drop tower use. The optical set-ups are complicated, the laser systems are incompatible with fibre optics, and some form of cryogenic Dewar or refrigerator is necessary.

Advances in near-infrared diode laser fabrication technology and the concurrent development of optical fibres for these lasers have led to their use in drop towers [4]. Since near-infrared absorption line strengths for overtone and combination vibrational transitions are weaker than the mid-infrared fundamental bands, wavelength modulation spectroscopy (WMS) techniques [5–8] can be applied to increase detection sensitivity and allow the measurement of the major combustion gases.

In the first microgravity species measurement, Silver *et al* [4] mounted a fibre-coupled laser at the top of the NASA Lewis 2.2 s drop tower and piped the light through a single-mode fibre to the drop rig. A 1×8 fibre splitter divided the light into eight channels that directed the laser beam across a methane or propane diffusion jet flame. The light beams were recaptured by a set of gradient index lenses, coupled back into separate fibre optic lines, and transmitted back to detectors and electronics in the instrument package. In these experiments a 6 mm diameter fibre cable (containing the nine optical fibres) fell with the drop rig. Using separate detection and demodulation channels, spatial and temporal (up to 20 Hz) maps of water vapour and methane concentrations were obtained at differing heights in the flames.

While this apparatus was useful from a demonstration standpoint, several drawbacks needed attention before useful scientific measurements could be obtained. First, eight lines of sight are somewhat insufficient for detailing the spatial profiles of a gas. Second, multiple detection channels operating in parallel are both expensive and present a challenge for accurate calibration. As a result, a newer scanning system was developed and is presented here. The primary characteristic of this new system is that it contains a single detection channel and achieves 'continuous' spatial resolution by scanning the laser beam across the flame region, then directing this beam onto a single detector. Thus spatial measurements are converted into a temporal data series. The true spatial resolution is limited only by the beam diameter and width of the sweep. In these experiments the beam is focused to about 1 mm diameter and scans across a region up to 4 cm wide.

Table 1. Comparison of vertical cavity surface emitting lasers (VCSELs) and distributed feedback (DFB) diode lasers.

	VCSEL	DFB
Wavelengths available (nm)	760–940	680–2000
Temp tuning ($cm^{-1}\,{}^{\circ}C^{-1}$)	-1	-0.4
Current tuning ($cm^{-1}\,mA^{-1}$)	~ 2	~ 0.025
Current limit (mA)	15	150–200
Wavelength range (cm^{-1}) tuned by current	5–15	0.5–2
Beam shape	Circular	Astigmatic
Beam divergence (FWHM)	10–20°	$40^{\circ} \times 60^{\circ}$
Typical detector	Si	InGaAs

The only drawback of this scanner approach is that the detection bandwidth is greatly increased over the fixed eight-channel instrument. Complete spectra must be obtained at each spatial point with a goal of making a full spatial measurement at $\sim$10 Hz. This is achieved by the use of high-speed analogue-to-digital converters coupled to digital signal processing (DSP) electronics, described in the next section. These dedicated devices permit rapid data acquisition with good amplitude resolution. The results of preliminary experiments using this system for the measurement of molecular oxygen in candle and solid thin sheet flames are discussed. Finally, current progress and future directions for diode laser-based diagnostic systems are presented.

3. Absorption methods

3.1. Diode lasers

As a class, diode lasers are ideal spectroscopic light sources for absorption measurements of gases under microgravity conditions. These all-solid state devices are very rugged and compact, and have low requirements for electrical power. They can be readily coupled with optical fibres for remote operation and can emit single-mode (single-frequency) light at milliwatt intensity levels. An important feature of these lasers is that they can be wavelength tuned at very high rates (up to a few gigahertz), permitting modulation and detection at very high bandwidths.

Diode lasers used in this study include distributed feedback (DFB) InGaAsP devices for near-infrared wavelengths (1200–2000 nm) and GaAlAs vertical cavity surface emitting lasers (VCSELs) that emit in the near visible (760–940 nm) spectral region. While both types are single-mode devices, DFB fabrication is a more mature technology and these lasers are available with fibre optic pigtails and optical isolators. Comparative properties of these lasers are shown in table 1.

The laser wavelength is controlled by a combination of temperature and injection current control. The lasers are mounted on thermoelectric coolers and the laser wavelength can be coarsely tuned by varying the laser temperature. Fine tuning is accomplished by tuning the injection current, for which the output wavelength has a linear response. As will be discussed below, the VCSEL is particularly attractive for local gas temperature measurements as it can be tuned over a wider range of wavelength, encompassing multiple absorption lines of the gas of interest.

3.2. Basic theory

The absorption of light by a gas is governed by the Beer–Lambert relation which states that the transmitted light intensity (I) through an absorbing sample of path ℓ with absorber number density n is proportional to absorbance, α,

$$I = I_0 \exp(-\alpha) \tag{1}$$

where

$$\alpha = S(T)g(\nu, T, P)n\ell \tag{2}$$

and $S(T)$ is the absorption line strength (units of cm^2/molecule cm^{-1}), $g(\nu, T, P)$ is the normalized molecular absorption line shape function and I_0 is the initial laser intensity. In the Doppler-broadened limit, which is a good approximation for measurements at high combustion temperatures and at pressures of one atmosphere or less, the line shape function is Gaussian in nature and independent of pressure. At low temperatures and at pressures of one atmosphere or more, the line shape scales linearly with pressure and is Lorentzian in nature. At intermediate temperature and pressure combinations, the line shape is described by a Voigt profile [9], which is a convolution of the Doppler and Lorentzian functions.

In the case of weak absorbances ($\alpha \ll 1$), equation (1) can be expanded and expressed as

$$\Delta I / I_0 = \alpha \tag{3}$$

where $\Delta I = I_0 - I$.

3.3. Wavelength modulation spectroscopy (WMS)

The greatest advantages of optical absorption spectroscopy are that the resulting signal is *linear* in concentration of the absorbing species and is *quantitative*. As expressed by the Beer–Lambert law, the signal is directly proportional (with a single system calibration constant) to the concentration. The difficulties of utilizing direct absorption for small absorbances is that one is trying to measure a small difference between two large numbers and that near dc these signals are noisy due to inherent laser source noise.

WMS shifts the detection bandwidth from dc, where measurements are limited by this excess ($1/f$) noise, to frequencies where laser-induced detector shot-noise is the limiting factor [10]. This method involves superposition of a small modulation at frequency f on the diode laser injection current. Typically, the amplitude of the current modulation is chosen so that the induced wavelength modulation is comparable to the width of the spectral feature under study. As the laser beam traverses the sample, optical absorption by the target gas converts some of the wavelength modulation into amplitude modulation of the laser intensity. This induced amplitude modulation occurs at the modulation frequency f and its integral harmonics, nf. Phase-sensitive electronics are then used to demodulate the detector photocurrent at a selected harmonic of the modulation frequency (typically $n = 2$). By implementing this technique at sufficiently high frequencies, excess laser noise is minimal and detector-limited sensitivity is achieved. Our studies have shown that detection frequencies as low as 50 kHz are often sufficient to achieve these objectives, although the optimum frequencies are laser dependent. More detailed descriptions of WMS theory are available in references [5–7] and [10].

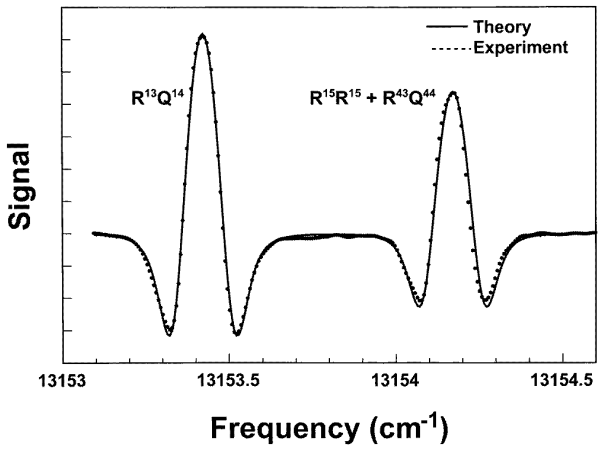

Figure 1. Oxygen spectrum in room temperature air. 31 cm absorption path, 10 Hz bandwidth.

A spectrum of two adjacent O_2 absorption lines near 760 nm is shown in figure 1. For comparison, a theoretical spectrum computed from known spectroscopic and physical parameters (path, composition of air, laser properties, etc) is illustrated. The agreement between these spectra demonstrates the convergence of experiment and theory, with a 1 Hz bandwidth noise level equivalent to 1×10^{-6} absorbance.

The second harmonic ($2f$) signals produced by WMS are directly proportional to absorbance, but the factor relating the $2f$ signals to absorbance at line centre is best determined by direct experimental calibration. Ideally, such a calibration is done by comparing a direct transmission measurement of absorption with a $2f$ measurement for the specific absorption feature under study or by calibrating the $2f$ signal directly to a known gas concentration. For water and methane, the former approach is used; for O_2, the latter method is used in room-temperature air.

Wavelength modulation spectra are normalized to I_0 to correct for misalignments, obscuration, degrading of optics, etc. As the diode laser wavelength is repetitively scanned across the gas absorption feature, the full absorption profile is acquired and fitted to calibration or reference spectra for determination of the absolute absorbance. From this the gas concentration is uniquely determined using equation (2).

Examination of WMS noise sources reveals that signal-to-noise ratios (SNRs) generally vary inversely with the square root of the bandwidth, so that high bandwidth detection can be obtained with moderate degradation of the signal. Due to the high frequency modulation capabilities of diode lasers, detection bandwidths approaching megahertz rates are feasible for major species such as water and methane that have large line strengths. To achieve very fast time response, it is preferable not to scan the wavelength across the entire line shape (requiring typically 100–250 individual measurements), but rather to position the laser at line centre and perform a single measurement for each time period. This is possible using dual-modulation WMS spectroscopy

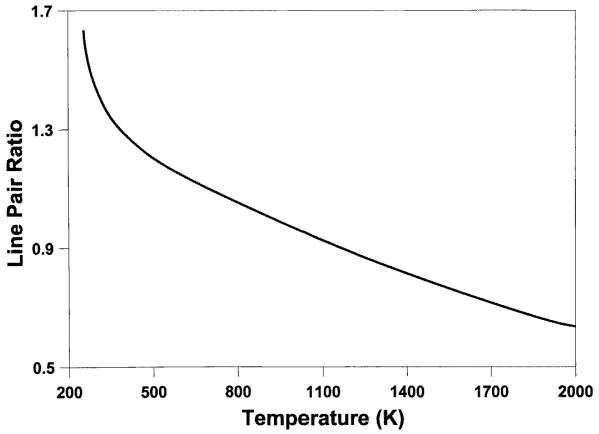

Figure 2. Peak height dependence on temperature for O_2 lines shown in figure 1.

[11], a variation of WMS where a second lower frequency modulation Ω of the wavelength ($\Omega < f$) oscillates between the two downward lobes of the $2f$ line shape. A second demodulation at 2Ω provides an output proportional to the peak-to-trough height of the $2f$ line shape without having to scan the laser centre wavelength. Using dual-modulation WMS, two-dimensional imaging at frame rates of 20 Hz is possible.

3.4. Concentration, mole fractions and temperature

The absolute gas concentration is obtained from either the peak height or line shape fit of the WMS spectrum. The corresponding mole fraction is

$$X_i = n_i RT/P_{tot} \tag{4}$$

where R is the ideal gas constant and P_{tot} the total pressure. The local gas temperature is needed to determine mole fraction. While in theory this can be accomplished from a careful fit to the full line shape, in reality such a determination is highly inaccurate due to the relative insensitivity of line shape to temperature and to complications arising from self-broadening effects for species such as water vapour. A better approach is to recognize that the line strength S is independent of pressure and depends only on temperature. Thus the ratio of the peak heights of two or more lines depends only on their (known) molecular parameters and on T.

The absorption line strength S at any temperature T can be expressed by

$$S(T) = S(T_0)\frac{Q(T_0)}{Q(T)}\exp\left[\frac{-hcE_r}{k}\left(\frac{1}{T}-\frac{1}{T_0}\right)\right] \times\left(\frac{1-\exp(-hc\nu/kT)}{1-\exp(-hc\nu/kT_0)}\right) \tag{5}$$

where h is the Planck constant, k is the Boltzmann constant and c the speed of light. $S(T_0)$ is the line strength at reference temperature T_0, which for example could be the HITRAN [12] tabulated room temperature value, 296 K. The Q terms are total internal partition functions (equal here to $Q_{\text{vibration}}Q_{\text{rotation}}$) and are readily computed [13]. The exponential term containing E_r (the total rotational energy of the molecular quantum state absorbing the light) accounts for the rotational Boltzmann populations at T and T_0. The last term accounts for stimulated emission which, at the laser frequencies and temperatures of interest, can be neglected.

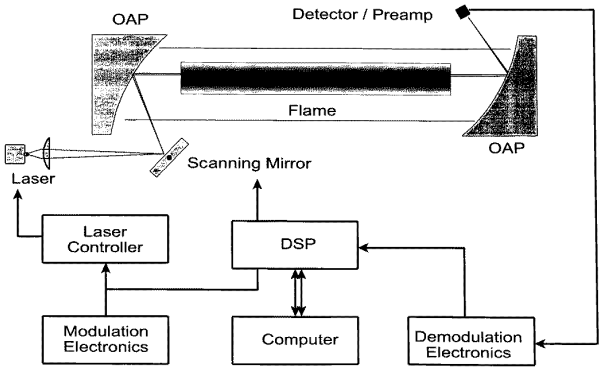

Figure 3. Overall layout of diode laser scanner system.

In taking the ratio of two nearby lines having different rotational energies, one obtains

$$\text{Ratio} = \frac{S_1(T_0)}{S_2(T_0)}\exp\left[\frac{-hc\Delta E_{rot}}{k}\left(\frac{1}{T}-\frac{1}{T_0}\right)\right] \tag{6}$$

where ΔE_{rot} is the difference in lower state rotational energy between the two absorption lines. For example, the ratio of the heights of the pair of lines shown in figure 1 has the temperature dependence illustrated in figure 2. The sensitivity of temperature measurements using this line pair is best at temperatures below 2000 K where absolute line strengths are relatively strong. The line pair peak heights change rapidly with temperature and their ratio tracks nearly linearly above ~600 K. Optimal line pairs can be chosen depending on the temperature range of interest.

3.5. Limitation of optical absorbance methods

Two points should be noted concerning the determination of mole fraction and concentration. First, since the line shape function and line strength are temperature dependent, the conversion of absorption to concentration requires some estimate of temperature. Concentration uncertainties can be minimized by selecting an absorption line whose combined line strength and shape are relatively insensitive to temperature over the range of temperatures expected. However, the computation of mole fraction requires an accurate value for T. If gas temperature itself is a measurement objective and is not available independently, it can be obtained by the ratiometric techniques described above.

The second important point is that optical absorption is a line-of-sight technique, and is best applied to one-dimensional systems which exhibit constant (or nearly so) profiles along this line-of-sight, such as slot burners, solid sheet combustion or pool fires. When the concentration profile is not uniform across the line-of-sight, tomographic reconstruction can be used to invert the data to obtain spatial profiles. For non-turbulent axisymmetric flames, Abel transforms can be used to obtain radial profiles [14]. This approach was taken in our previous early microgravity research on jet diffusion flames [4] and was used in the candle measurements described later in this paper.

3.6. WMS detection limits for combustion gases

Sensitivity for detecting a particular gas depends on its concentration, temperature, spectroscopic properties and availability of lasers at the desired wavelength. Table 2 outlines the expected detection levels for selected major gas phase flame species. Detection sensitivities are listed at an absorption level achievable with a detection bandwidth of 1 Hz. Higher bandwidth measurements degrade as the square root of the bandwidth. Presently, only DFB lasers are available in the near-infrared spectral regions, and VCSELs are limited to use for detecting absorbers below 1 μm.

For water vapour, the first line listed in table 2 is very strong at room temperature and has been used in most prior studies. Combustion measurements should use the latter line since its line strength is much greater at high temperatures, thereby lessening the effect of moisture in any external room-temperature air path from interfering with the flame signal. Table 2 also indicates that the hydroxyl radical should be observable. Note that molecular oxygen is a particularly weak absorber and is included because of its great importance in controlling ignition and extinction processes. Despite the difficultly in measuring O_2, this work is an attempt to demonstrate that under optimum circumstances, such a measurement is possible.

3.7. Optical detection of O_2

Although vibrational bands of O_2 are infrared-*inactive*, electronic bands in the near-infrared spectral region can be used as the basis of an absorption diagnostic. The $v' = 0 \leftarrow v'' = 0$ band of the magnetic dipole transition from the $X^3\Sigma_g^-$ ground electronic state to the excited $b^1\Sigma_g^+$ state occurs in a spectral region that is easily accessed by commercial GaAlAs diode lasers operating in the 750 to 780 nm range. This band system of oxygen has been well characterized spectroscopically; precise values for line strengths, self-broadening, and air-broadening coefficients are available [12, 15–16].

4. Experimental details

Figure 3 shows the configuration of the laser diode scanning system in schematic form. The system comprises four components: (1) the optical scanning system containing the laser, scanner, mirrors, detector and preamplifier all mounted on a frame for which the absorption path can be varied; (2) stand-alone computer and digital signal processing (DSP) boards; (3) an analogue electronics box containing all laser control, WMS and signal processing circuitry; and (4) the dc computer power supply. The system is powered by sealed, rechargeable lead-acid batteries on the 2.2 s drop tower rig. Power loading is relatively high, drawing 7 amps at 28 V dc, which depletes the batteries in less than 30 min.

The laser is mounted on a thermoelectric cooler to maintain its operating temperature regardless of ambient temperature fluctuations. The laser beam is collimated by an anti-reflection coated aspheric lens to a diameter of <1 mm, and is pointed at a scanner mirror that is positioned at the focus of an off-axis paraboloidal mirror (OAP) so that all rays reflected by the OAP are parallel to one another. As the

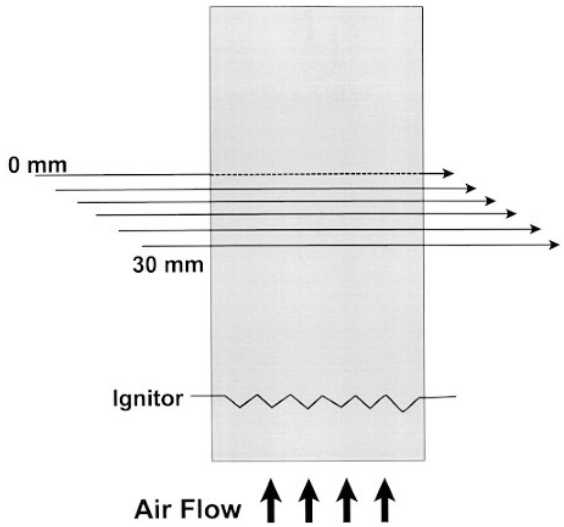

Figure 4. Solids combustion set-up.

beam is swept by the scanner, it tracks in parallel lines across the flame. After traversing the flame, a second OAP refocuses the laser beam onto a single silicon photodetector. The end result of this process is that data acquired sequentially in time can be used to obtain spatially resolved line-of-sight measurements across the flame. Inherent in this design is that the total optical path for all spatial positions is identical.

To be compatible with the 2.2 s drop tower, this system is self-contained. A rugged, passive backplane unit holds a stand-alone Pentium computer card, Data Translation DT3801 DSP board, scanner circuit and hard drive. The electronics unit contains the laser controller, modulation and demodulation boards, and all I/O circuitry. The entire optical and electronics package fits on a single platform in the drop rig.

The angle of the scanner is controlled by a programmable voltage ramp generated by the DSP unit. This ramp is constructed so that the laser beam reflected off the OAP rasters linearly in time across the absorption region. As the absorption region is being spatially scanned by the laser beam, the controller rapidly sweeps the laser wavelength across the absorption feature. The sweep waveform includes a linear rise with a hyperbolic tangent reset function permitting the laser to rapidly return to its starting wavelength without causing ringing in the signal processing electronics. A full spectrum (280 spectral bins) is obtained during the time in which a single spatial resolution element ($\sim$1 mm) is traversed. Data collected during the linear portion of the ramp are used in the final analyses.

WMS detection is accomplished by modulating the laser wavelength at 500 kHz and detecting the $2f$ (1 MHz) component of the photodiode. A custom preamplifier separates the ac ($2f$) from the dc (I_0) signals. The ac signal is demodulated using an I & Q mixer that provides two outputs: one in phase with the 1 MHz local oscillator and the second 90° out of phase. Data are recorded using the analogue inputs to the DSP unit and stored on either a solid state drive or hard drive designed for use in a laptop computer. The electronic circuitry for modulation and demodulation is similar to that described in [4]. The DSP board controls all timing, ramps

Table 2. Expected gas concentrations and detection sensitivities.

Gas	λ (nm)	Maximum expected concentration (cm^{-3})†	Detection sensitivity (cm^{-3})‡
Oxygen	760	8.9×10^{17}	6×10^{16}
Water	1392.53	8.9×10^{17}	4×10^{14}
	1392.85		9×10^{13}
Carbon dioxide	1550	4.5×10^{17}	6×10^{16}
Hydroxyl	1450	5×10^{16}	6×10^{12}
	1393.34		8×10^{13}
Methane	1651	4.5×10^{17}	2×10^{14}

† Stoichiometric methane–air flame at 1 atm, 1500 K.
‡ Minimum detection sensitivity $\alpha = 3 \times 10^{-6}$, $\ell = 2$ cm.

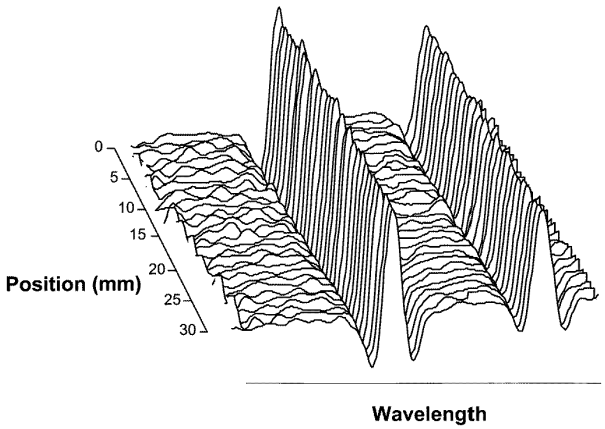

Figure 5. Typical spectral profiles versus position for oxygen.

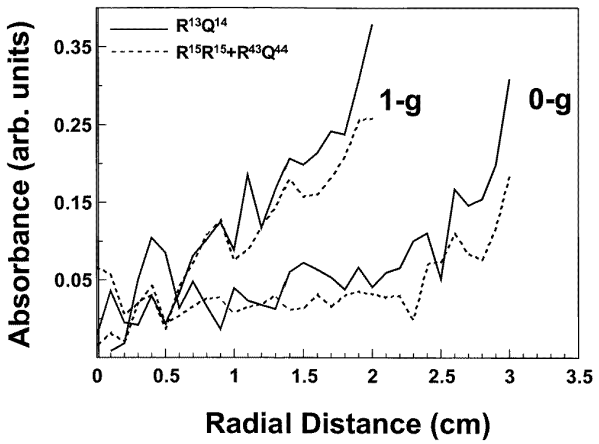

Figure 6. Comparison of absorbance profiles in a candle flame for microgravity and normal gravity.

and triggering of the system. Numerical processing of the data and normalization to I_0 are carried out in post-drop analysis.

As shown in figure 4, the solids combustion set-up comprises a thin metal frame to which an 8.5 cm wide cellulose sheet (Kimwipe EX-L) is taped. A Kanthal ignitor coil is mounted in physical contact with the bottom of the sheet (and covered with a $1/8''$ high strip of nitrocellulose paper wetted down by acetone) to assure quick and even ignition of the sheet. A small fan below the frame provides a concurrent flow of air to promote migration of the flame front

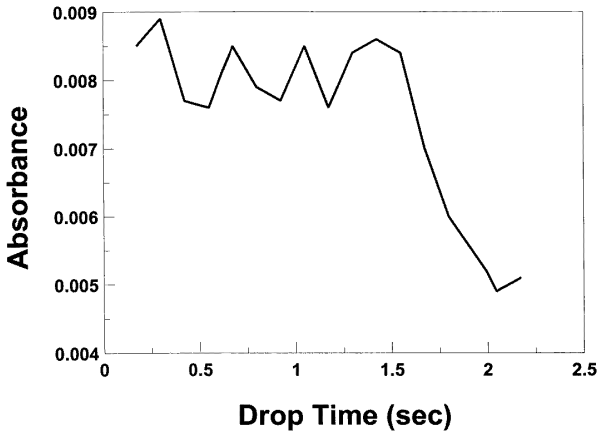

Figure 7. Spatial average of solids combustion peak absorbance in zero gravity.

upwards from the ignition point. For candle measurements, a small birthday cake candle is inserted into the optical path.

The goal of these experiments is to make quantitative measurements of molecular oxygen concentrations in concurrent flows and candle flames with a time and spatial resolution sufficient to resolve questions concerning the relative effects of diffusion and kinetic limitations on observed combustion properties. As such, constraints for the experimental system are defined as follows. The spatial resolution is 1 mm across a 3 cm flame region, defining a 30-point spatial scale for either line-of-sight or radial (via an Abel transform) measurements. The time resolution of each spatial map is 8 Hz. Finally, sufficient sensitivity to detect molecular oxygen ranging from ambient concentrations to depleted levels at combustion temperatures is required.

5. Results and discussion

5.1. Sensitivity

Normal and zero-gravity experiments were performed in the 2.2 s drop tower at NASA Lewis Research Center. These included measurements using a candle and a thin cellulose sheet. Since each spatial map was taken at 8 Hz and at 30 spatial locations, 240 spectra were acquired, processed and stored each second. The effective detection bandwidth was about 70 kHz. An example of raw spectral data is shown in figure 5. These data were phased, normalized to I_0 and co-aligned.

One complication in the data analyses is that O_2 is present in the optical path external to the flame (i.e. in the room air). This introduces a nearly overwhelming contribution to the observed signal that must be subtracted to determine the portion contributed only by the flame. Not only is the external path (in this system, at least) much larger than the flame lengths, but the effect of temperature on number density (equation (4)) favours the room-temperature signal. Thus very large SNRs are required in order to successfully subtract out the room-temperature portion of the signal.

A sense of the SNR can be seen from these data. We note that the co-alignment step is necessary only for the VCSEL and arises from its extreme response of wavelength to changes in the injection current. Both the starting wavelength on each repetitive sweep and the precise sweep rate are not constant, forcing the scan rate and starting wavelength of each scan to be adjusted individually. A best fit to the raw data (air path unsubtracted) is used to determine these parameters and correct the data accordingly before external path subtraction. Co-alignment is not an issue for DFB laser measurements. In future work, laser controllers having better current and/or temperature stability (i.e. more suited to working with VCSELs) should be used.

5.2. Candle flames

Experiments on a small candle were carried out in normal gravity and microgravity. The results are compared in figure 6. The long external path in these experiments (as compared with the flame diameter of only a few centimetres) resulted in flame region spectra having a poor SNR. To improve this we co-averaged spectra over all drop times (beginning after the initial transient to zero gravity). Since the candle is axially symmetric, an Abel inversion of the data converts the observed projections through the flame into radial absorbances. The reduced gravity data clearly show a wider flame. This is in agreement with the videotape recording.

The signals for the line pair are too noisy to extract exact temperatures, but qualitatively one can see that at the edge of the flame the line pair ratios are, as might be expected, near 300 K. In these experiments we selected a line pair optimized (in signal strengths) for temperatures of 1200–1500 K. In retrospect, a better range would have been 600–1000 K, since O_2 disappears in the flame front and residual O_2 is not expected to be present in the hotter flame zones.

In this study, the flame was ignited before the drop and the transition to zero gravity induced flame wobble, degrading the data. Future work will include post-drop ignition and a much shorter mirror separation to reduce the effect of external air on the measurements.

5.3. Solid sheet combustion

An 8.5 cm wide thin solid sheet was burned in zero gravity under a small concurrent flow of air. As shown in figure 4, the laser beam traversed a 30 mm wide path perpendicular to the sheet and the flame passed through this plane after ignition. Since the total laser intensity I_0 at the detector was recorded, obscuration of the laser beam by smoke and/or the flame is observed. In accordance with a video recording of this drop, the smoke is slightly ahead of the flame and partially obscures the laser at about 1.5 s. Smoke obscuration is strongest closer to the sheet. Although I_0 is diminished by the smoke, the absorbance measurements are unaffected by this phenomenon since the overall signals are normalized to changes in I_0 (see equation (3)).

The absorbance map for O_2 remains fairly constant up to about 1.7 s, when a precipitous drop is observed due to the passage of the flame front. A spatial average over all positions is shown in figure 7; the drop in absorbance is clearly visible. In this experiment, the laser frequency shifted just before the drop so that only one of the (normally) two absorption lines was observed. As a result, we could not ascertain a temperature map.

6. Conclusion and future directions

Progress in quantifying gas temperatures and concentrations under microgravity conditions using diode laser absorption is advancing rapidly. This technique has been demonstrated in a variety of 0–g flames, detecting water vapour, methane and molecular oxygen. The high bandwidth capabilities of WMS permits one- and two-dimensional images of a species to be obtained quickly enough to see the effects of transition from normal to zero gravity in drop towers as well as to observe the development of flame structures while in 0–g.

While the present system is reasonably compact, advancements in micro-processing technology now allow significantly smaller and less power-hungry instrumentation. We are presently developing both one- and two-dimensional imaging systems which use stand-alone DSP super-processors. The one-dimensional system is only about $5\,\text{cm} \times 10\,\text{cm} \times 15\,\text{cm}$ in size and replaces all of the electronics currently used. Power requirements drop to below 30 W. This is made possible by using a fully digital approach to WMS where a modified square wave modulation waveform, rather than an analogue sine wave, is used [17–18]. The DSP unit can now generate and process all modulation, ramping and scanning waveforms, as well as analyse and store the data without the need for a separate computer board.

A further improvement uses the high bandwidth capabilities of WMS. Two-dimensional images of species concentrations can be captured using a dual-scanner system and a very fast A/D-coupled DSP system [19]. Images of 100×100 pixels can be captured at 20 Hz rates by combining dual-modulation WMS [11] with the dual scanner. First, a high-speed two-channel D/A waveform generator outputs waveforms up to 10 MHz. This board provides both the modulation (for the diode laser) and demodulation (for detection) waveforms. A custom built high bandwidth mixer/detector board is followed by a high-speed (10 megasamples per second (MSPS)) 12-bit digitizer for the demodulated signal. For this imaging system, the total sample load is $\sim$0.6 MSPS. DSP on-board can hold up to 8 megasamples or 266 frames. Diode laser-based gas detection systems are suitable for inclusion in the International Space Station. They could be used as compact, low cost sensors for microgravity combustion research, air quality management and fire detection. Direct monitoring of ambient air properties, such as temperature and the presence

of hazardous gases, could assure fire safety. The flexibility and interchangeability of diode lasers combined with the widespread capabilities of absorption measurements make this approach a strong candidate for use in the Modular Combustion Facility aboard the Space Station.

Acknowledgments

This work was performed under NASA Contracts NAS-25981, NAS3-26553 and NAS3-96018. The authors thank Dr Paul Greenberg and Dr Nancy Piltch of NASA Lewis Research Center for their expertise, support and assistance in this research.

References

[1] Greenberg P S 1992 *Second International Microgravity Combustion Diagnostics Workshop (15–17 September 1992)* NASA Conference Publication 10113, NASA Lewis Research Center, Cleveland, OH, pp 61–6
[2] Hinkley E D 1972 *Opto-Electron.* **4** 69–86
[3] Silver J A and Stanton A C 1987 *Appl. Opt.* **26** 2558–66
[4] Silver J A, Kane D J and Greenberg P A 1995 *Appl. Opt.* **34** 2787–801
[5] Wilson G V H 1963 *J. Appl. Phys.* **34** 3276–85
[6] Reid J and Labrie D 1981 *Appl. Phys.* B **26** 203–10
[7] Silver J A 1992 *Appl. Opt.* **31** 707–17
[8] Bomse D S, Silver J A and Stanton A C 1992 *Appl. Opt.* **31** 718–31
[9] Hui A K, Armstrong B H and Wray A A 1978 *J. Quant. Spectrosc. Radiat. Transfer* **19** 509–16
[10] Cooper D E and Warren R E 1987 *J. Opt. Soc. Am.* B **4** 470–80
[11] Bomse D S 1991 *Appl. Opt.* **21** 2922–4
[12] Rothman L S *et al* 1992 *J. Quant. Spectrosc. Radiat. Transfer* **48** 469 (1996 HITRAN and HITEMP CD-ROMs)
[13] Herzberg G 1950 *Molecular Spectra and Molecular Structure II. Spectra of Diatomic Molecules* (New York: Van Nostrand Reinhold)
[14] Dasch C J 1992 *Appl. Opt.* **31** 1146–52
[15] Ritter K J and Wilkerson T D 1987 *J. Molec. Spectrosc.* **121** 1
[16] Ritter K J 1986 *PhD Dissertation* University of Maryland, USA
[17] Fried A, Drummond J R, Henry B and Fox J 1991 *Appl. Opt.* **30** 1916–32
[18] Coffey M, Mankin W and Harrigan J 1999 Private communication National Center for Atmospheric Research
[19] Kane D J 1999 *Fifth International Microgravity Combustion Workshop (18–20 May 1999)* NASA Lewis Research Center, Cleveland, OH, submitted for publication